

This is the peer reviewed version of the following article:

Active vibration control of a composite sandwich plate / Zippo, Antonio; Ferrari, Giovanni; Amabili, Marco; Barbieri, Marco; Pellicano, Francesco. - In: COMPOSITE STRUCTURES. - ISSN 0263-8223. - STAMPA. - 128:(2015), pp. 100-114. [10.1016/j.compstruct.2015.03.037]

Terms of use:

The terms and conditions for the reuse of this version of the manuscript are specified in the publishing policy. For all terms of use and more information see the publisher's website.

10/02/2025 07:35

(Article begins on next page)

Accepted Manuscript

Active Vibration Control of a Composite Sandwich Plate

Antonio Zippo, Giovanni Ferrari, Marco Amabili, Marco Barbieri, Francesco Pellicano

PII: S0263-8223(15)00210-X

DOI: <http://dx.doi.org/10.1016/j.compstruct.2015.03.037>

Reference: COST 6307

To appear in: *Composite Structures*



Please cite this article as: Zippo, A., Ferrari, G., Amabili, M., Barbieri, M., Pellicano, F., Active Vibration Control of a Composite Sandwich Plate, *Composite Structures* (2015), doi: <http://dx.doi.org/10.1016/j.compstruct.2015.03.037>

This is a PDF file of an unedited manuscript that has been accepted for publication. As a service to our customers we are providing this early version of the manuscript. The manuscript will undergo copyediting, typesetting, and review of the resulting proof before it is published in its final form. Please note that during the production process errors may be discovered which could affect the content, and all legal disclaimers that apply to the journal pertain.

Active Vibration Control of a Composite Sandwich Plate

Antonio Zippo^{a,*}, Giovanni Ferrari^b, Marco Amabili^b, Marco Barbieri^a,
Francesco Pellicano^a

^a*Department of Engineering “Enzo Ferrari”, University of Modena and Reggio Emilia,
Via Vignolese 905/B, 41125 Modena, Italy*

^b*Department of Mechanical Engineering, McGill University, Macdonald Engineering
Building, 817 Sherbrooke Street West, Montreal, QC, Canada H3A 0C3*

Abstract

Active vibration control of a free-edge rectangular sandwich plate is proposed and tested. The experimental setup consists of a honeycomb panel having a carbon-fiber reinforced polymer (CFRP) outer skins and a polymer-paper core, subjected to an orthogonal disturbance, due to an electrodynamic exciter and controlled by Macro Fibre Composite (MFC) actuators and sensors. MFC patches consist of rectangular piezoceramic rods sandwiched between layers of adhesive, electrodes and polyamide film. The MFC actuators and sensors are controlled by a programmable digital dSPACE[®] controller board. The control algorithm proposed in this paper is based on the Positive Position Feedback (PPF) technique and is successfully applied with different combinations of inputs/outputs (Single Input Single Output, MultiSISO, Multi Input Multi Output) in order to control the first four normal modes. The control appears to be robust and efficient in reducing vibration in linear (small amplitude) and nonlinear (large amplitude) vibrations regimes, although the structure under investigation exhibits a relatively high modal density, *i.e.* four resonances in a range of about 100Hz. The control strategy allows to effectively control each resonance both individually or simultaneously.

*Corresponding author

Email addresses: antonio.zippo@unimore.it (Antonio Zippo),
giovanni.ferrari@mail.mcgill.ca (Giovanni Ferrari), marco.amabili@mcgill.ca
(Marco Amabili), mark@unimore.it (Marco Barbieri),
francesco.pellicano@unimore.it (Francesco Pellicano)

Keywords: Active Vibration Control, experimental, composite structures, plates, nonlinear dynamics

1. Introduction

Experimental studies in nonlinear dynamics play a key role and have a high relevance both to validate numerical and theoretical models and to highlight and discover complex behaviours of mechanical systems and structures. Nowadays, the increasing use of new materials (composite carbon fibre, etc.) makes more important to refine the testing procedures due to the intrinsic nonlinear properties and their innovative applications. In such work an accurate study of a thin walled structure was carried out to better understand the nonlinear dynamics of shells and plates; once the behaviour has been defined experimentally a further step has been made to solve the problems due to nonlinear vibrations, applying different kinds of active vibration control. Indeed, today's industry makes an extended use of thin walled composite structures, especially in the field of aerospace. Composite laminated structures are characterised by an extremely high specific stiffness, together with a good flexibility in achieving complex shapes. As a typical example, the bodywork and elements of the frame of racing cars and bikes can be mentioned. Typically loose fixings and fastenings further contribute to the development of large amplitude vibrations, which can result in noise disturbance for passengers, functional problems or even sources of danger.

In general, the simplest way to reduce vibrations is to design the system with additional damping, by using special materials or adding physical damping devices. This approach is called passive vibration control (or redesign) and is a very well developed subject area for linear vibration problems, see Soong et al. [1] and Lam et al. [2]. Passive techniques, such as the classical tuned mass damper (see Den Hartog [3] for a description relating to linear vibration) have been extended to nonlinear systems with good results [4]. Passive solutions are often preferred in practice as they can be built into the system and there is no control element, which eliminates any issues with stability or robustness. However, for a growing class of structures for which reduced weight and flexibility are important features, passive redesign is not an effective design solution. Active control systems are becoming desirable, since they do not require the increase of mass due to dampeners, stiffeners and absorbers; moreover they can adapt to disturbances deterministically unknown, varying with time or even to large amplitude phenomena. Examples

of practical active vibration control systems include active engine supports in vehicles and active vibration isolation systems for propeller aircraft. Depending on the problem, increasing stiffness and damping or isolating the structure are the most common solutions to obtain a vibration reduction. Stiffening the structure consists of shifting the resonance frequency beyond or over the frequency band of excitation. Increasing damping consists of reducing the resonance peaks by dissipating the vibration energy. Isolation consists of preventing the propagation of disturbances to sensitive parts of the systems. Several techniques are well known to increase the damping of a structure (passive vibration control) with fluid dampers, eddy currents, elastomers or hysteretic elements, or by transferring kinetic energy to dynamic vibration absorbers [3].

Another common method is the use of transducers as energy converters that transform vibration energy into electrical energy that is dissipated in electrical networks, or stored (energy harvesting). Formerly, semi-active devices, also called semi-passive, (passive devices with controllable properties) have been used. The magneto-rheological fluid damper and piezoelectric transducers with switched electrical networks are examples.

Such techniques have very high rate of effectiveness, but when high performance is needed active control is the best choice. Active vibration control involves a set of sensors, a set of actuators and a control algorithm ; the design of the system implies many issues such as the sensors and actuators configuration and how to assure stability and robustness. The power requirement is crucial to define the size of the actuators and the cost of the setup.

Compared to other control problems, structural control has a number of specific features:

1. the systems under investigation generally have a large number of degrees of freedom (DOFs) and a large number of modes;
2. in general attention must be paid to the fact that the high-frequency modes outside the frequency band of interest influence the position of the open-loop zeros of the system;
3. many structures involved in structural control are lightly damped ($\zeta \sim 0.001$ to 0.05).

The latter point means that the stability margin of the uncontrolled modes is small, sometimes very small, and that they are subject to spillover,

which means that the control system always tends to destabilise the flexible modes just outside the control bandwidth: the only margin against spillover instability is provided by damping of the residual modes. The combination of a large number of modes with a small stability margin calls for specific control strategies emphasising robustness, with respect to the residual dynamics (high-frequency modes) and also with respect to the changes in the system parameters. Control systems with collocated (dual) actuator/sensor pairs exhibit special properties which are especially attractive in this respect. The recent results regarding the forced nonlinear vibrations of composite sandwich plates, the newest and up-to-date technologies developed in the field of active control systems and the new smart materials structures allow to perform an innovative research. In Ref. [5, 6] it's described the vibration characterisation of a carbon-epoxy / honeycomb panel with free edges, in linear and nonlinear field. In such articles a complete modal analysis, obtained by advanced techniques, can be found together with a nonlinear study of damping. The damping values of composite structures undergoing large amplitude vibrations are not easily predictable, therefore they could result a problem for the effectiveness and stability of a control technique.

Free boundary condition is used in this work because is an interesting application for/to active control algorithms, since it reduces the influence of temperature, assembly and non-ideal boundary conditions, but at the same time includes rigid modes of vibration.

Piezoelectric technology is today dominant in the realisation of sensors and actuators for the control of mechanical vibrations, especially in the case of thin-walled shells and plates; it features lightweight elements and good frequency characteristics, the drawback is a limited actuation force. The advances in real-time embedded controllers, versatile and with extremely high performances make affordable the application of a modal Positive Position Feedback by means of piezoelectric actuators affordable. This has in fact proven effective and promising in the case of continuous aerospace structures, with respect to traditional negative position feedback and feedforward (be it adaptive or not), see Kumar [7], Carra et al. [8], Zilletti et al. [9].

The technique of Positive Position Feedback was extensively studied by Kwak [10] and Friswell [11]. The PPF is particularly effective if focused on chosen frequencies and modes, although, in Ref. [12] it is shown how the operation of one actuator can be extended to the control of more than one mode, and has good characteristics against spillover if it is correctly applied. Moreover, the PPF is easy to design if damping ratios are well known and

it can be extended to the nonlinear field. The effect of PPF active control is to add a "virtual damping" to the system at the desired targeted frequency. It is therefore goal of this study to obtain both a broadband vibration reduction, an example is the MPPF proposed by Mahmoodi et al. [13], and the suppression of single or multi vibration modes, see Omid [14]. The application to carbon-epoxy / honeycomb panels with free edges seems interesting from an industrial point of view. This is especially true if the applied sensors and actuators are inexpensive, lightweight and easily bondable. The optimal positioning of the piezoelectric patches can moreover be determined by a common finite element analysis; strains of the composite structure can actually suggest where to put the transducers used for the modal control. Fanson and Caughy [15] proposed the PPF control method on the modal displacement signal, where the controller is very effective in suppressing specific vibration modes, thus, maximising damping in target frequency band without destabilising other modes.

2. Positive Position Feedback

In the single DOF case, to the one degree of freedom vibrating system a compensator is added, sharing a second order equation - in modal coordinates. The two equations of system and compensator are:

$$\ddot{\xi} + 2\zeta\omega\dot{\xi} + \omega^2\xi = g\omega^2\eta \quad (1a)$$

$$\ddot{\eta} + 2\zeta_f\omega_f\dot{\eta} + \omega_f^2\eta = \omega_f^2\xi \quad (1b)$$

ξ, ζ, ω are modal displacement, modal damping ratio and natural frequency of the structure respectively η, ζ_f, ω_f are the degree of freedom (e.g. force), damping ratio and natural frequency of the compensator, while g is the gain of the compensator. The global system is made of two coupled second order systems and it is absolutely stable for values of gains $g < 1$ [10, 16]. The compensator implies active damping if η is -90° out of phase with respect to ξ , at ω . For lower frequencies it adds active flexibility and for higher frequencies active stiffness. Therefore the compensator is usually tuned at $\omega_f = \omega$, in order to have the desired mitigation of vibration amplitude.

$$H(s) = \frac{\omega_f^2}{s^2 + 2\zeta_f\omega_f s + \omega_f^2} \quad (2)$$

At frequencies above ω_f the slope of the transfer function amplitude is negative and very steep ($-40dB/octave$), so it reduces the problem of spillover for

vibrations at higher frequencies. On the contrary, at frequencies below ω_f the bode diagram of $H(s)$ has an amplitude of 0 dB, which can cause spillover, that implies to the undesired effect of control on modes outside the frequency band of interest. More precisely, spillover happens if control actuators excite unwanted modes and spillover if control transducers measure unwanted modes. Robustness against instability was also studied in Ref. [17], particularly, if the sensor and the actuator are collocated nearby in Ref.[18, 19]. The resulting damping ratio of the controlled system is:

$$\zeta_c = \zeta + \frac{g}{4\zeta_f} \quad (3)$$

The choice of g and ζ_f is constrained by delicate considerations because it influences the final Bode diagram of the controlled system. Compared to negative position feedback, the PPF has a similar behavior, with the main advantage of a better performance towards spillover at higher frequencies. The roll-off rate of the PPF is actually $\frac{1}{\omega^2}$, while it is $\frac{1}{\omega}$ for the negative feedback. Although it is advised for lightly damped systems and well separated modes, in such paper, control spillover regarding higher frequencies than the observed ones is reduced.

The extension of a modally optimised control to nonlinear vibrations must contemplate the frequency shift of softening/hardening systems and the appearance of companion, subharmonic, superharmonic resonances. A common strategy is a linearizing module followed by a common linear algorithm. A PPF system could instead deal directly with weakly nonlinear vibrations.

In the practical implementation of positive position feedback control on a multiple degrees of freedom structure takes the form:

$$M\ddot{x} + C\dot{x} + Kx = C_a v_a \quad (4)$$

$$v_s = C_s x \quad (5)$$

where M , C and K are the mass, damping and stiffness matrices, x the displacement vector, v_a and v_s the actuator and the sensor voltage vectors, C_a and C_s the actuator and sensor participation matrices. Through the reduced order modal coordinates

$$x = Uq \quad (6)$$

where q is the generalized displacement vector and U the eigenvector matrix, the equation takes the reduced order modal form

$$\ddot{q} + 2Z\Omega\dot{q} + \Lambda q = \bar{B}_a v_a \quad (7)$$

$$v_s = \bar{C}_s q \quad (8)$$

3. Setup and system description

Passive vibration control methods are very effective at high frequencies, where more energy is into play, or in a narrow frequency range, where the target frequencies are well defined; however, they have often the disadvantage of added weight, adding mechanical complexity to the whole system and poor low-frequency performance. Active vibration controls have demonstrated the potential to circumvent many of these problems. Although the potential of active vibration control has been well known for many years, only recent advances in real-time digital signal acquisition and processing hardware and software have made these systems feasible. The purpose of active vibration control is to modify the system response in a desired manner, by means of a secondary vibration input applied to the structure. It's possible to identify four main components of an active vibration control system: the plant, the actuators, the sensors, and a controller. The plant represents the physical system to be controlled; it is important to note that the properties of the plant are modified by the presence of the actuators and the sensors, usually integrated by bonding or bolting. Error sensors plays a key role as they measure the system response while control actuators provide the necessary inputs to the plant in order to modify its response. The controller is the biting heart of the control, where a specific control algorithm is implemented in order to ensure that the controlled (or closed-loop) system behaves as required. The closed-loop system consists of the open-loop (uncontrolled) system dynamics combined with the dynamics of the controller. The arrangement of an active control system is usually based upon the physics of the system to be controlled and thus it is often application-dependent, see Beranek [20], therefore a special effort must be paid to built up an *ad hoc* setup: Figure 1 shows all the components of the present tests.

In the next subsections the relevant parts will be discussed.

Honeycomb carbon fibre sandwich panels

Honeycomb carbon fibre sandwich panels are important composite structures in aerospace applications as well as in high performance automobiles,

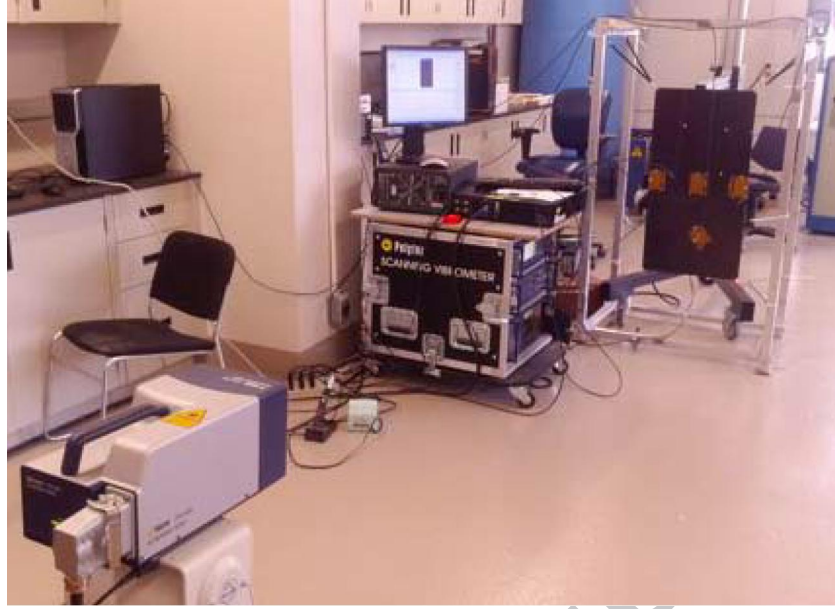


Figure 1: Overall setup

boats and wind turbines. Typically, a sandwich panel is characterised by a low stiffness, low density inner core enclosed by two stiff outer skins, as shown in Figure 2; the whole assembly is held together by a structural adhesive, e.g. epoxy glue. Outer skins are typically made of stiff carbon fibre or aerospace grade aluminium.

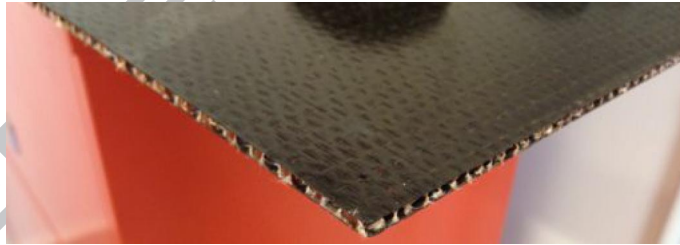


Figure 2: Honeycomb carbon fibre sandwich panel

A sandwich plate of 460 mm wide and 900 mm high was tested. The skins of the sandwich plate, shown in Figure 1, are made of Carbon/Epoxy composite with $0/90^\circ$ lay-up (the zero angle refers to the external layer, with fibres

parallel to the longer dimension). The thickness of each Carbon/Epoxy layer is 0.17 mm and its properties have been identified with a combination of static and dynamic tests, it was manufactured at the Structures and Composite Materials laboratory of McGill University using vacuum bag processing equipment, suitable for manufacturing sandwich plates with thin sections and large in-plane dimensions. In particular, the plate has a PLASCORE[®] PN2 aramid fiber paper core made of DuPont[®] Nomex paper with hexagonal cell dimensions $l = H = 4.5\text{mm}$, $t = 0.0762\text{mm}$, $\theta = 30^\circ$ and average core thickness of 2.92mm. Nomex is an aramid polymer similar to Nylon, which is flame-resistant and can be manufactured in paper sheet form, it is a good choice for the interior of aircraft cabins due to its high safety in the event of fire. An experimental characterisation of the mechanical vibrations of the sandwich rectangular plates was performed by means of no-contact laser Doppler vibrometers (Polytec PSV-400[®]) to reconstruct the normal modes by measuring a considerable number of points of the structure.



Figure 3: Panel backside and shaker

The punctual excitation of the structure is provided by means of a traditional electrodynamic shaker, Bruel and Kjaer Modal Exciter Type 4824[®], see Figure 3. The excitation point is located 75 mm far from the geometric center of the panel, and has been used both for the modes identification and as the external disturbance vibration (broadband, impulsive and sine) which the active control aims to reduce. The force applied by the shaker is measured by means of the force transducer Bruel and Kjaer Type 8203[®] (sensitivity $3.3pC/N$), between the shaker and the force transducer a stinger, made of harmonic steel, is interjected to reduce the effect of misalignments. The modal analysis, see section 4, has been performed in the relevant bandwidth where the active control will be involved to between 0-100 Hz, it shows a sequence of four vibration peaks in the frequency domain. A complete experimental modal identification was performed in order to obtain normal modes, see Table 1, natural frequencies and damping ratios. The resulting four flexural normal modes perfectly match with numerical results. The values of the damping ratios satisfy the condition of light damping. The plate shows a weakly nonlinear hardening behaviour starting from excitation amplitudes around 8.5 N and visible nonlinear jumps from vibration amplitude 1.5 times the thickness.

Boundary conditions

The aim of the active control experiments is the reduction of vibration of a 3.6mm laminated sandwich plate with free boundary conditions. It resulted more practical to glue the active control elements (both actuators and sensors) on the smoother side of the panels. On the same side a reference vibration can be measured by no-contact laser vibrometer; the excitation instead is applied on the opposite surface. Free boundary conditions were easily realised with a suspension on elastic cords and nylon wires, subjected to a modest tension, just enough to support the weight of the panel itself without introduce any relevant external tensile forces. Particular attention was paid to create a symmetric wiring links to reduce the effects of the rigid body motions of the plate. An aluminium frame has been designed to hang the panel in vertical position, which has been chosen so that the weight of the piezoelectric elements and the relevant cabling does not burden while the plate vibrates. Tests have been performed to verify that the wires tensile forces do not affect the plate dynamics.

MFC patches

Macro Fiber Composites (MFC) made of PZT (lead zirconate titanate) fiber in stack configuration have been used as actuators and sensors in this research. Several kind of actuators can be adopted depending of system requirements as amount of control force, moment, strain, or displacement, and depending also on physical constraints such as size, mounting requirements, etc. . Actuators are generally classified into two main categories: fully active actuators, used in this work, applying a secondary vibrational response to the structure (i.e., can add energy to the structure) and semi-active actuators, passive elements that can be used to adaptively adjust the mechanical properties of the system (i.e., *do not feed energy into the structure*).

As discussed in [21], piezoelectric transducers consist of material that expands or contracts when an electric field is applied. By applying an oscillating voltage to the piezoelectric element, it oscillates at the same frequency of the input. Three major types of piezoelectric material are readily available:

- a ceramic form such as PZT (Lead Zirconate Titanate), which has relatively high control strain but is brittle;
- a polyvinyl form such as a PVDF (Polyvinylidene Difluoride), which is flexible but has less control strain for the same configuration
- a piezoelectric rubber, which is useful for underwater applications

Piezoelectric material is configured in the two main forms of *stack* and *wafer*. Piezoelectric stacks are configured so that when a voltage is applied across the electrodes, the stack usefully expands in its length (common considered 3 – 3 axis). Stack arrangements are thus suitable for actuators in vibration isolation in the two configurations of parallel and series; for a given applied voltage V the net static displacement δ of the piezoelectric ceramic actuator in the parallel configuration can be calculated from:

$$\delta = \frac{d_{33}V + F/K_a}{1 + K/K_a} \quad (9)$$

where d_{33} is the strain constant of the piezoelectric material (d33 effect: elongation) in the 3 – 3 axis, K is the external spring stiffness, K_a is the actuator stiffness ($K_a = E_a A_a / L_a$, where L_a, A_a , and E_a are the actuator length, cross-sectional area, and Young's modulus, respectively); F is the external load force. Note that equation 9 can be used as the basis of an approximate

dynamic analysis, as discussed in [22] by Fuller.

The significant advantage of the piezoelectric stack is that it can provide high force; however, its displacement is limited (when compared with electrodynamic actuators), which implies that its use is primarily in series-active isolation implementations. The other common form of piezoelectric actuator is the wafer, in this form the transducer usefully strains in its thin transverse axis (3–1 or 3–2) when a voltage is applied across the electrodes. Piezoelectric elements are arranged to create pure bending, indeed, the surface-mounted collocated actuator with a perfect bending layer (which is a good approximation if the glue layer is thin) effectively applies a line moment to the structure at the boundaries of the actuator.

The Macro Fiber Composite (MFC) are chosen as actuators and sensors, they consists of rectangular piezoceramic rods sandwiched between layers of adhesive, electrodes and polyimide film. The electrodes are attached to the film in an interdigitated pattern which transfers the applied voltage directly to and from the ribbon shaped rods. This assembly enables in-plane poling, actuation and sensing. MFC P1 type (d33 effect) elongates utilising the in-plane effect, will elongate up to 1800ppm if operated at the maximum voltage rate of -500V to +1500V.

MFC thin rectangular patches, produced by Smart Materials Corp.[®][23], were bonded by epoxy glue (LOCTITE[®] E-120HP) whereas the electric connection has been made with a silver conductive epoxy glue by MG Chemicals with $0.017 \Omega \cdot cm$ electrical resistivity . These elements can act as actuators as well as strain sensors, or even act as energy harvesters; in this application, two different models were used separately as actuators (M8557-P1 see Figure 4a) and sensors (M8507-P1 see Figure 4b). To place the piezoelectric sensors and actuators in the ideal position, in order to interact optimally with the target modes, a finite element model has been developed using Patran-Nastran[®] to find the maximum and minimum strain in the plate.

The sandwich plate has been modelled as a laminated layered structure: the external layers and the internal core were defined as transversely equivalent isotropic material with no variation along the thickness. The frequencies and the mode shapes obtained by this analysis were very close to the experimental ones and perfectly match the theoretical model of the plate, see Table 1. The placement of each pair of sensor-actuator was chosen by a modal criterion. Each pair of sensor and actuator physically was physically placed side by side along the longer dimension, according to the concept of quasi-perfect nearby collocation and its intrinsic stability characteristics. The final

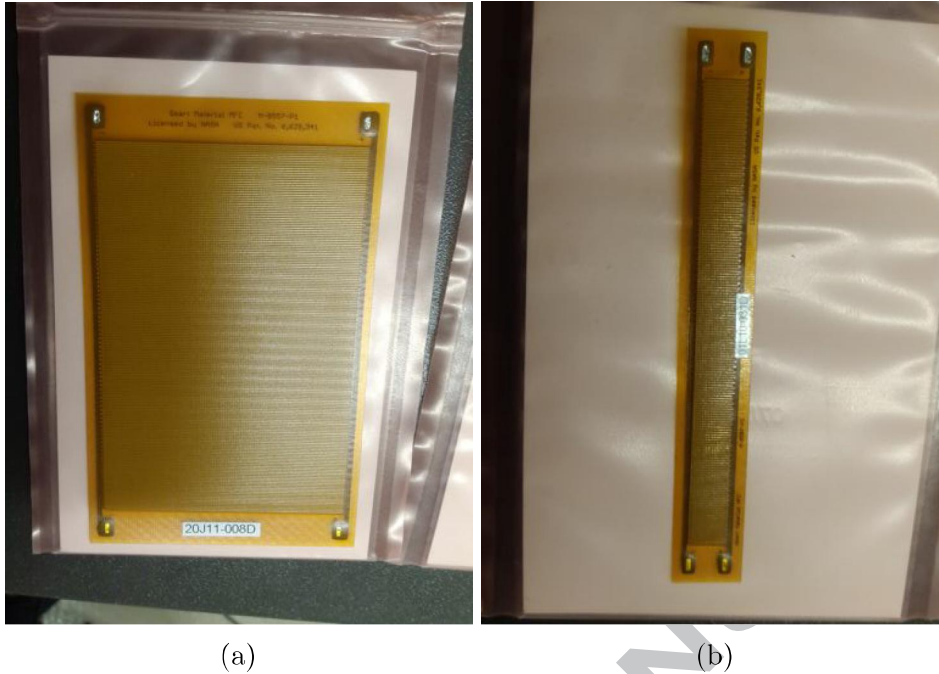


Figure 4: (a) actuator (M8557-P1); (b) sensor (M8507-P1)

configuration for MIMO control consists of two sensors and four actuators, see Figure 5: one collocated pair of sensor–actuator (element 2) is placed in the geometrical center of the plate and its direction is parallel to the longer side of the plate. Two actuators (element 1 and 3) are parallel to this couple and are collocated on the symmetry line of the rectangular plate parallel to the shorter side. Another collocated pair (element 4) is glued in the bottom half of the plate, 200 mm from both the bottom and the right side of the panel. These two patches are roughly 30 degrees tilted from the direction of the shorter side of the panel.

Due to the location and the direction, the relationship between piezoelectric elements and normal modes of vibration is:

1. Element 2: it measures and acts on the mode II and, to a lesser extent, mode I.
2. Element 1 and 3: they excite mainly the II and III mode and to a lesser extent also the IV mode.

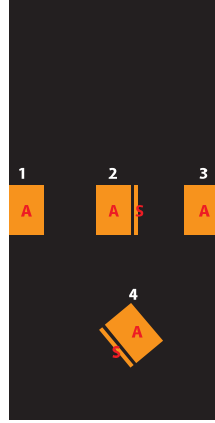


Figure 5: PPF MIMO Control, patches configuration

3. Element 4: it measures and excites the I and III mode and, to a lesser extent, the IV.

The resulting configuration is shown in Figure 14.

dSPACE[®] real-time controlling system

The real-time data acquisition system by dSPACE[®] has been installed configuring software and hardware connections and was used to design several kinds of control algorithms. dSPACE[®] hardware consists of a compact controller board (DS1103 PPC) with a programmable real-time processor. The interface board has a wide variety of inputs and outputs channels and is connected to a Windows[®] PC workstation by means of an ethernet cable for commands communication and with an optical cable for the transfer of the acquired data. The Real-Time Interface (RTI) dSPACE[®] is linked to the VHDL code generated from the algorithm implemented in a Simulink[®] environment and is embedded into the control board after the compiling, placing and routing on the FPGA processor of the control board. 36 analog-to-digital (A/D) channels are present as well as 8 digital-to-analog (D/A) one: A/D and D/A channels are synchronisable. The Matlab/Simulink[®] environment allows to develop a simulated model of the system and the subsequent application to the real plant. RTI manages both continuous-time and discrete-time signals; therefore, the Simulink model has to take into account the problems due to digitalisation. Figure 6 shows the hardware equipment.

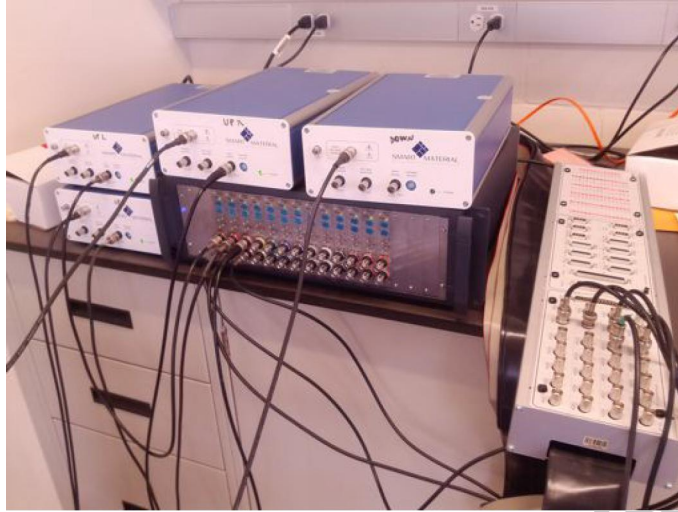


Figure 6: Power amplifiers, digital filter and dSPACE® control board

Additional conditioning hardware

The dSPACE® Control Board works with signal ranges up to ± 10 V. This range is adequate for the piezoelectric patches used as sensors, while it is completely inadequate to drive the actuators, since their maximum operating voltage is required to control the composite panel (-500 V, $+1500$ V). TREK High Voltage Power Amplifiers, Model PA05039, by Smart Materials® was used to amplify the signal by a factor of 200. The input and output range of the amplifier units are designed to perfectly match the requirements of the piezoelectric actuators and to generate a voltage of $-500/+1500$ V. As common for piezoelectric application, the operational limits are not symmetric; therefore, the signal generated by the dSPACE® controller and the Simulink® code must not exceed $-2.5/+7.5$ V, to prevent excessive output a saturation block has been embedded in the output blocks and an hardware limits has been settled for the tests. In order to exploit all the available voltage amplitude an offset of $+2.5$ V was considered in the Simulink® algorithms. The effect of static preload due to the constant piezoelectric patch contraction has been considered and it was verified that it did not cause any significant modification on the vibrational behavior of the plate. Moreover, an analog low-pass filter (KEMO® CardMaster 21.255G [24]) is interjected between the dSPACE® output and the input of the amplifiers, in order to

cut unwanted high harmonics, due also to digitalisation and noise.

4. Experimental modal analysis

In linear systems, each vibration mode has an associated resonance (or natural) frequency which occurs at a clearly defined resonance peak. At, or near, the point of resonance, the motion of the linear system will be dominated by the vibration mode which correlates to that particular resonance peak – if only the specific mode is present this is called a pure modal response. In multi-degree-of-freedom linear systems this means that the steady-state response reduces to a series of single-degree-of-freedom harmonic oscillators for each mode. These oscillators are defined by the modal displacement of the resonant mode. In nonlinear systems, the shapes of the resonance peaks are often amplitude-dependent or distorted due to nonlinear effects such as those associated with hardening or softening behavior.

Here, an experimental modal analysis has been performed, a grid of 45 points was defined and by means of the laser vibrometer the response has been measured for all the points of the grid. The experimental data have been used to reconstruct the modal shapes with a dedicated Matlab script, see Table 1, while in Figure 7 it is shown the average FRF broadband signal that has been obtained; the modes of the plates can be easily associated to the resonance frequencies of the average FRF.

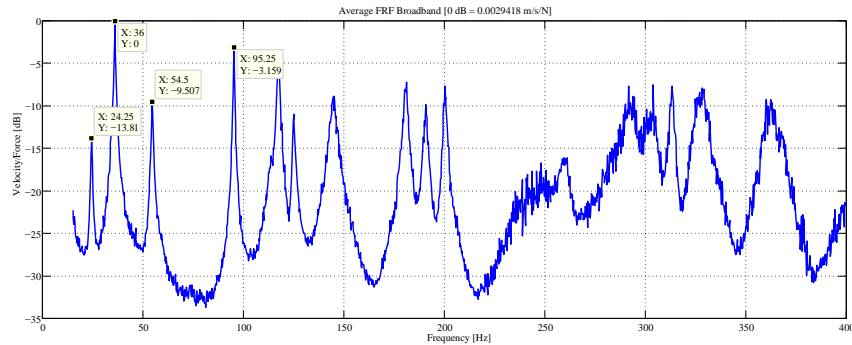
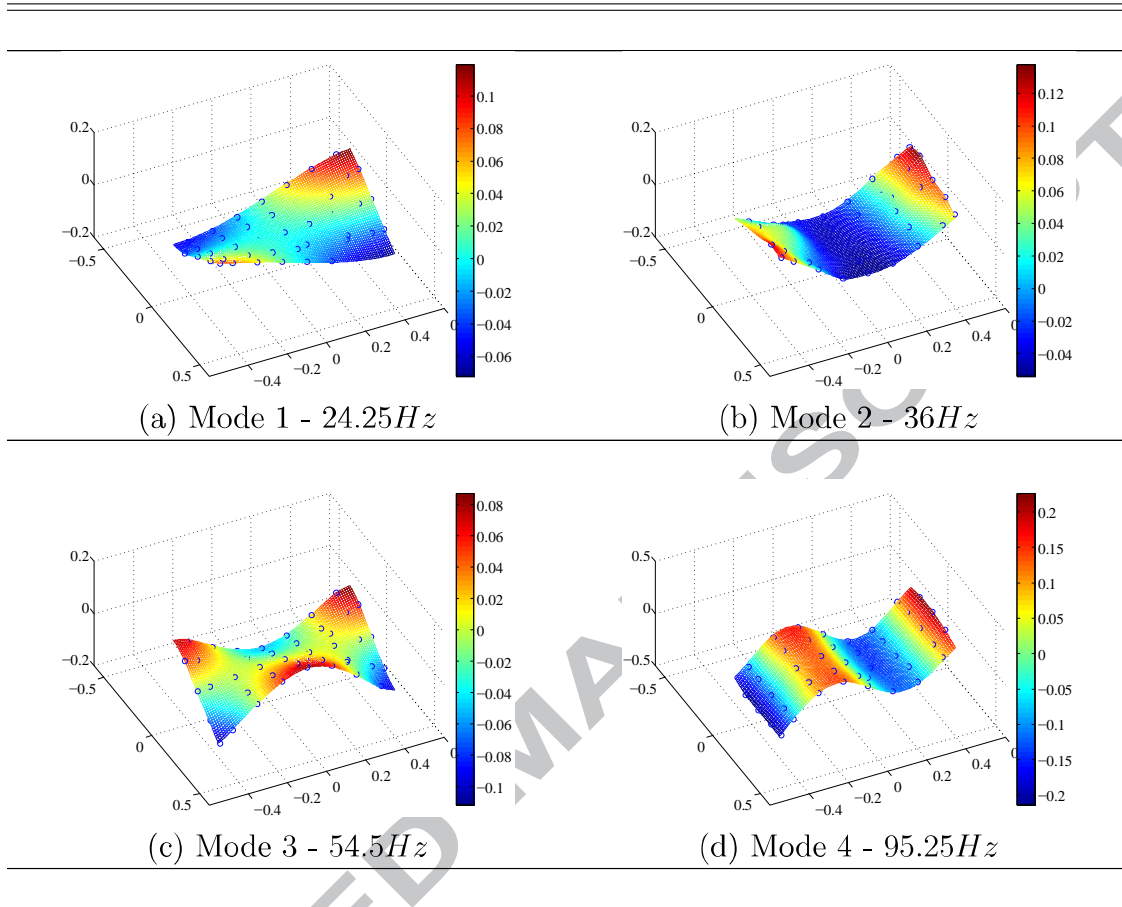


Figure 7: Average FRF - Broadband signal

Table 1: Experimental modal shapes



5. Experimental PPF Active Control

The PPF has been designed on the basis of linear FRF, in this section of the application in linear field will be shown. The PPF algorithm is intrinsically modal. In a collocated control system, the actuator and the sensor are attached to the same DOF. Moreover, they must be dual, a force actuator must be associated with a displacement (or velocity or acceleration) sensor, and a torque actuator with an angular (or angular velocity) sensor, in such a way that the product of the actuator signal and the sensor signal represents the energy (power) exchange between the structure and the control system. Such systems have very interesting properties and have been studied in many

papers. Positive position feedback (PPF) was proposed to solve this problem by Fanson et al. in [15] and by Goh et al. in [25].

The second-order PPF controller consists of a second-order filter

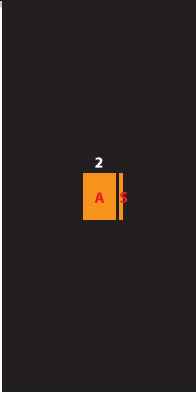

$$H(s) = \frac{-g}{s^2 + 2\zeta_f \omega_f s + \omega_f^2} \quad (10)$$

where the damping ζ_f is usually rather high (0.5–0.7), and the filter frequency ω_f is chosen to target a specific mode. The negative sign in $H(s)$, which produces a positive feedback, is the origin of the name of this controller. Considering the typical root loci, when the PPF poles are targeted to a single mode with respect to ω_f , it can be seen that the whole locus is contained in the left half-plane, except for one branch on the positive real axis; this part of the locus is reached only for large values of g , which are not used in practice. Therefore, PPF can be regarded as unconditionally stable.

5.1. PPF SISO Control

In the SISO configuration, see Table 2, one collocated pair of actuator-sensor is used and tested for case 1 and case 2 arrangement. Each sensor drives the collocated nearby actuator by means of a PPF block algorithm tuned on a single natural frequency. The central pair (element 2) was used to control the second mode exclusively, while the bottom pair was targeted on the first, third and fourth mode.

Table 2: PPF SISO control: (a) configuration Case 1; (b) Case 2

configuration Case 1	configuration Case 2
	

Continued on next page

configuration Case 1	configuration Case 2
(a)	(b)

5.1.1. PPF SISO Case 1

The piezoelectric pair of patches (element 2) has been specifically targeted on the second mode, in Figure 8 the open-loop Simulink[®] block diagram is shown. A reduction of 21dB in correspondence of the second resonance mode is measured in all the grid points, in Table 3 are shown the top and bottom right corner points, it is important to note that the other modes are not effected at all by the action of the the control.

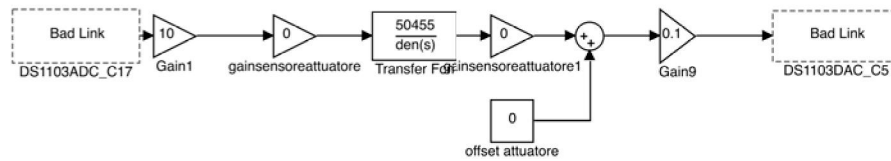
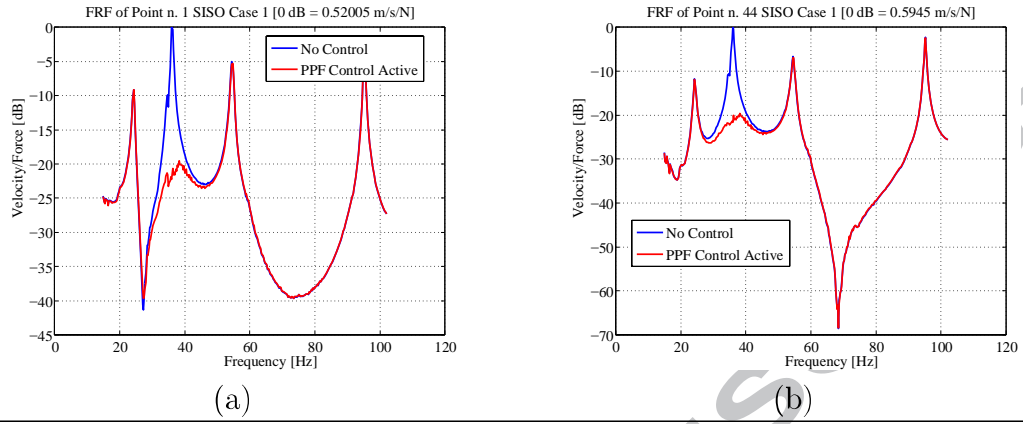


Figure 8: PPF SISO Case 1 Simulink[®] block diagram

Table 3: PPF SISO control Case 1



5.1.2. PPF SISO Case 2

In this configuration, shown in Figure 9, the lower actuator is positioned so as to work on the first, third and fourth modes. The results shown in Table 4 highlight a reduction for the third and fourth mode of approximately 5dB and 6dB; the first two modes are practically not affected, but while the second mode was not considered in the control, the first unchanged response of the first mode can be ascribed to its highly damped response.

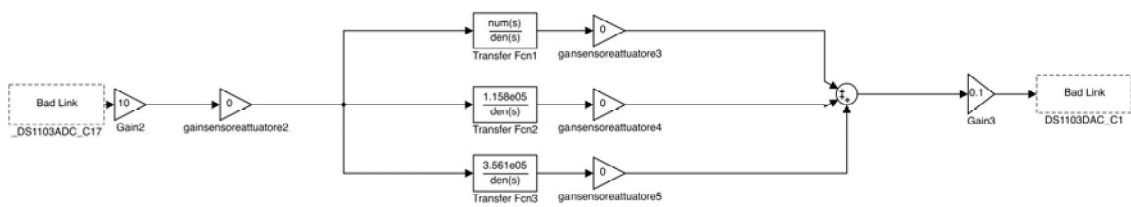
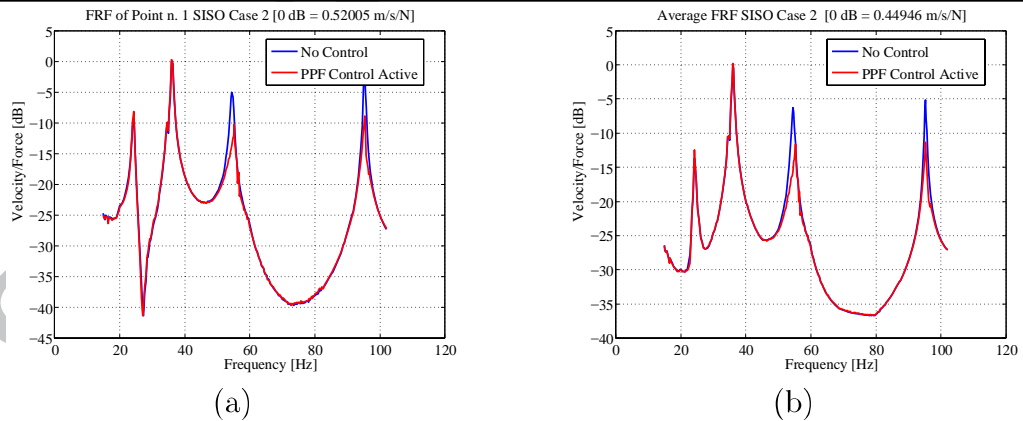


Figure 9: PPF SISO Case 2 Simulink[®] block diagram

Table 4: PPF SISO control Case 2



5.1.3. PPF SISO CASE 2 on 3rd mode

The PPF control have its main key point in the intrinsically modal attitude, in general the PPF algorithm works in a defined and limited frequency range close to the resonance frequency at which it is targeted; in our case the high modal density can induce modal interactions. In order to verify this hypothesis, a series of tests have been developed in order to check the possibility of modal interaction. In particular, for the element 4 (case 2 configuration) the third and fourth modes were controlled individually.

In Figure 10 the effect of SISO control for case 2 on the third mode is shown; with respect to a reduction of about 5dB on the third mode, it can be noted that also the first mode is lightly affected, so the extent of about 1dB.

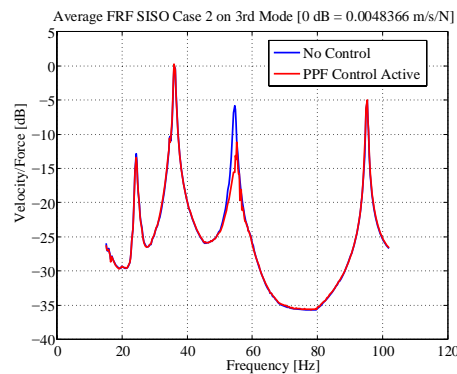


Figure 10: PPF SISO control Case 2, active only on third mode

5.1.4. PPF SISO CASE 2 on 4th mode

Repeating the same kind of test of the previous section on the fourth mode, see Figure 11, we found a reduction of 8dB, a really low disturbance decreasing, less than 1dB, is obtained on the 1st and 3rd modes.

5.2. PPF MultiSISO Control

The MultiSISO configuration (Figure 12) consists of the parallel use of the two SISO active controls. Figure 13 shows the patches configuration used for this test. In Table 5, the FRFs obtained applying the control are compared with the uncontrolled ones; while the 1st mode is substantially unchanged, the 2nd, 3rd and 4th modes decrease. The reduction of the second resonance

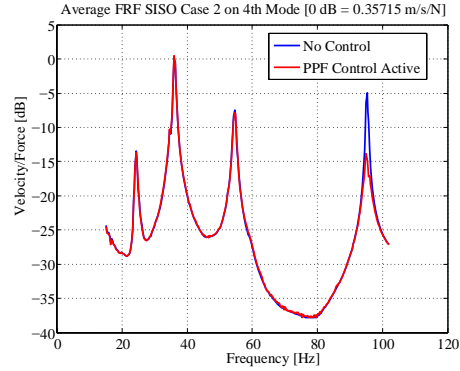


Figure 11: PPF SISO control Case 2, active only on fourth mode

peak is dominant with more than 20dB in the average FRF, see Table 5 (b), while the behaviour of other relevant points depends on the geometric position. The reduction of the third mode is 5dB, while it is for the fourth mode 8dB. In Table 5 (a) is shown the FRF of the bottom right corner of the plate.

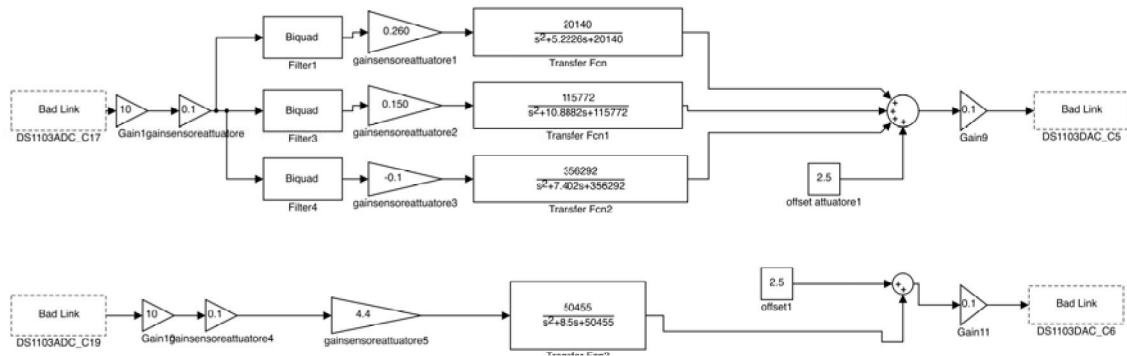


Figure 12: PPF MultiSISO Simulink® block diagram

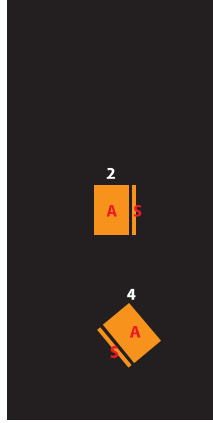
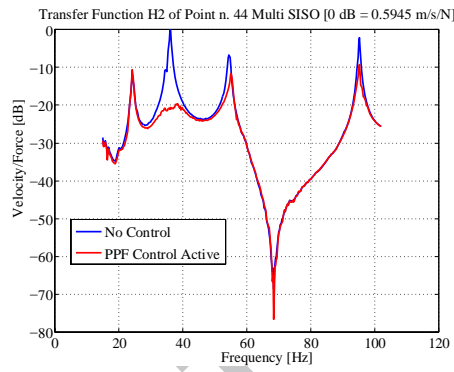
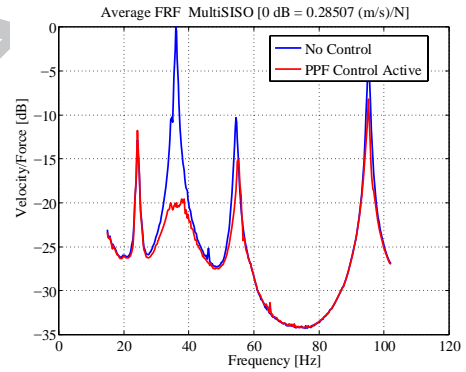


Figure 13: PPF MultiSISO Control, patches configuration

Table 5: PPF MultiSISO Control



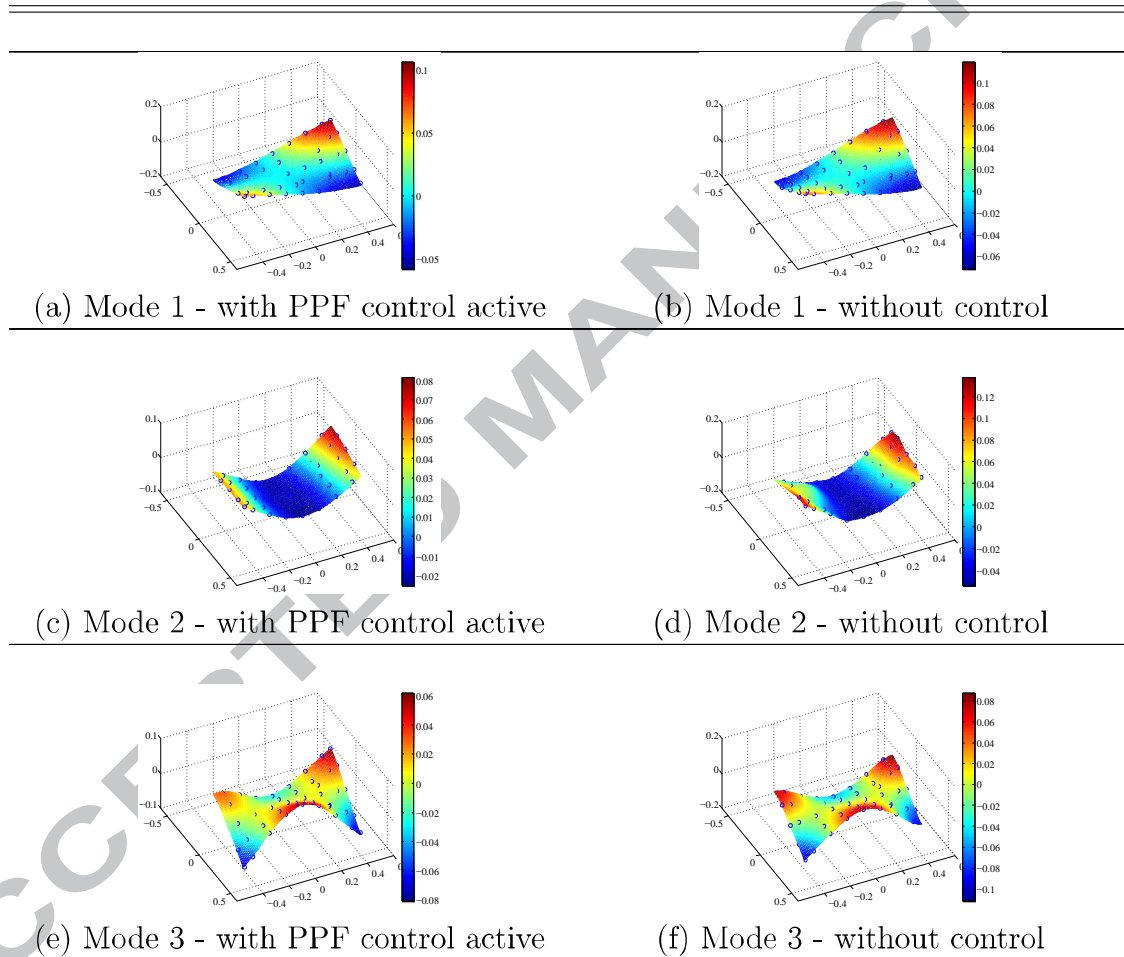
(a)



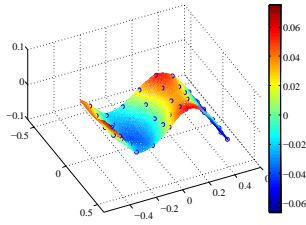
(b)

In Table 6, for the MultiSISO configuration a comparison of the FRFs with and without control for different points are shown. In order to prove the effective modal character of the PPF control the modal shapes, see Table 6, have been reconstructed from the experimental data and compared, considering the same external disturbance, in the presence or absence of MultiSISO control active. Moreover, the computation of the Modal Assurance Criterion, shown in Table 7, further proves the modal character of the PPF control.

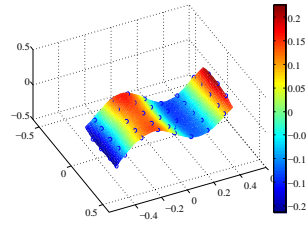
Table 6: Comparison of reconstructed modal shapes with and without PPF MultiSISO Control



Continued on next page



(g) Mode 4 - with PPF control active



(h) Mode 4 - without control

Table 7: MAC feedforward SIMO Control

	Mode 1	Mode 2	Mode 3	Mode 4
Controlled Mode 1	0.9936	0.1712	0.0020	0.0003
Controlled Mode 2	0.1580	0.9677	0.0214	0.0003
Controlled Mode 3	0.0201	0.0245	0.9620	0.0046
Controlled Mode 4	0.0000	0.0159	0.0000	0.8724

5.3. PPF MIMO Control

In the Multiple Inputs Multiple Outputs (MIMO) configuration, see Table 5, all elements are used, in particular the two piezoelectric sensors of element 2 and 4 are used for input signals and the four actuators are active. The complexity of algorithm and the consequent block diagram, shown in Figure 14, increase, causing major effort to calibrate the gains. In the block diagram only two actuators are represented because the signal directed to actuators 1 and 3 are identical or opposite to the signal to actuator 2. The sum of the two signals coming from the sensors is directed to each of the four control functions that the PPF feature for the first four modes. The actuators receive the sum of the outputs of the control functions as a pilot signal; the sign of the signal must be changed if, with regard to one specific mode used as reference, the signal from the sensor and the force of the actuator are located close to opposite antinodes. The two side actuators are mainly used to increase the force needed to control the second mode, that have the highest response at resonance; moreover, considering their location and the magnitude of the

second mode, their effect and the relative transfer functions are similar to each other and with respect to the central actuator. Because of this, just two actuators are included in the MIMO and the number of combinations drops to four instead of eight. The signals from the control blocks are then summed and sent to the actuators. The sums of the signals of the sensors and of the actuators are possible since the superposition principle is valid in the linear field. In Table 8 it is shown the effect of the MIMO active control on some relevant points and the average FRF of all the scanned points. An impressive disturbance reduction has been reached not only for the modes with higher responses but also for the others. The second mode has an average reduction of 20dB, the fourth of 15dB, while the third of 12.5dB and the first of 10dB.

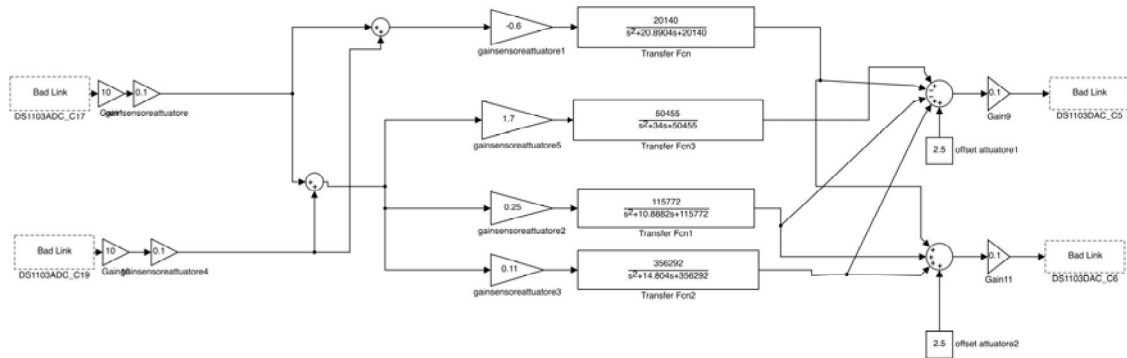
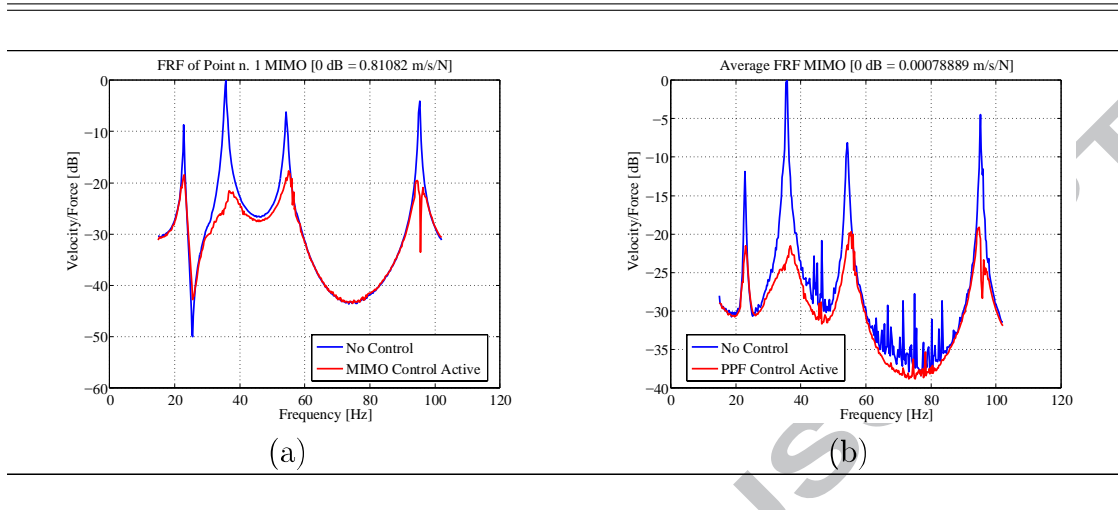


Figure 14: PPF MIMO Simulink[®] block diagram

Table 8: PPF MIMO Control



5.4. PPF Active Control in large vibration amplitude regime

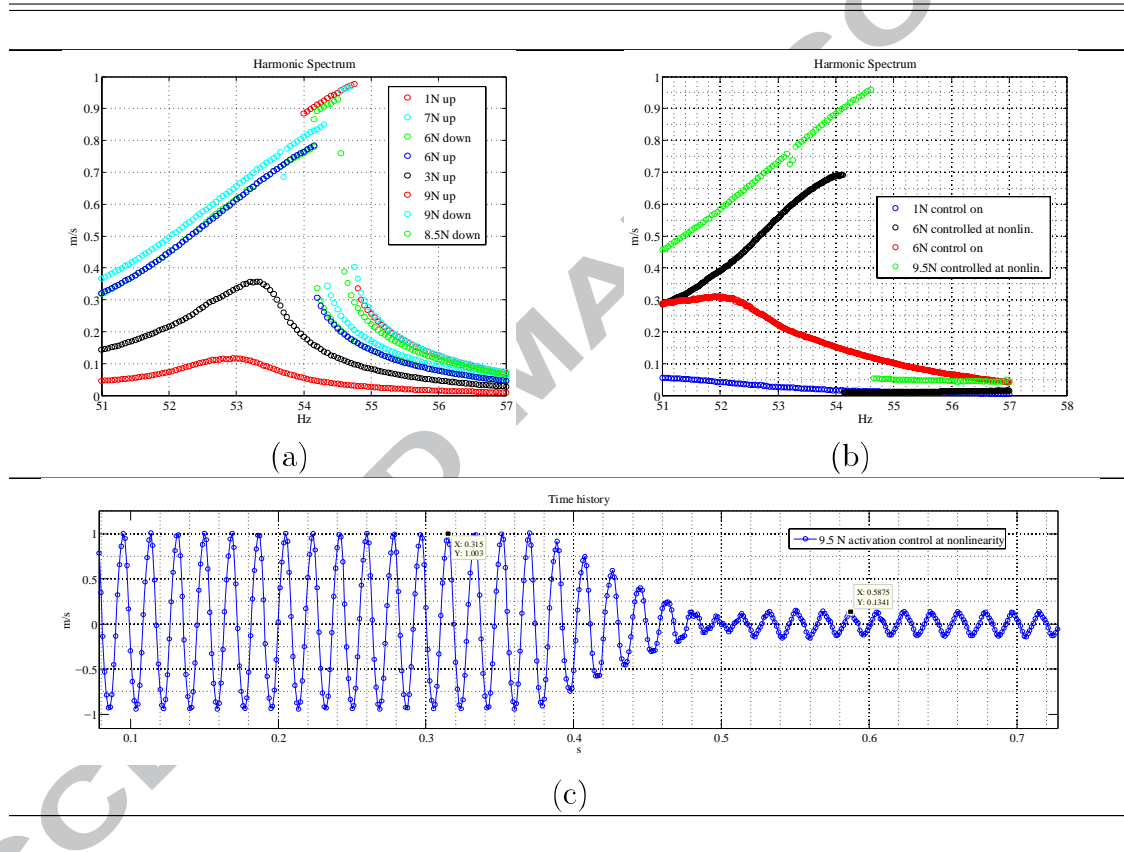
Considering the satisfactory results obtained with the MIMO configuration, it was decided to evaluate the present active vibration control in non-linear field.

First of all, a characterisation of the nonlinear behaviour of the plate has been carried out, in particular the third mode has been taken into account. A series of upwards and downwards sine sweeps at controlled forcing amplitudes have been performed between 51 and 57 Hz. The amplitude of the sweeps was varied by steps of 1 N. In Table 9 (a), an hardening behaviour is clearly highlighted with the resonance peak passing from 53Hz at 1N to almost 55Hz at 9N. Moreover, at 9N a jump between high and low amplitude state is present; Table 9 (b) shows tests at different force level carried out to verify the effectiveness of the active control in nonlinear regime: at 9.5N the active control was activated (green line) 0.2 Hz before the jump during an upwards sweep; the vibration passes from 1m/s to less than 0.1m/s. As also confirmed by the time history, Table 9 (c), the control acts in less than 0.1 seconds. The same tests were carried out with a 6N forcing load with satisfying results (black line); moreover the same test was repeated but activating the control from the outset at a forcing load of 6N (red line) and 1N (blue line).

It is to note that, the control activation during a fully developed nonlinear regime (Table 9b) cause a very strong reduction, leading the system to a

vibration state characterised by an amplitude notably smaller than that obtained with the control active from the beginning. One can object that at low amplitude, the system behaves linearly so there is no explanation of the different states obtained activating the control since the beginning or during the test (large amplitude). The explanation is in the time history, Table 9c, where it is clear that the low amplitude state still preserve a nonlinear character, as the wave is not sinusoidal but triangular. This issue will deserve a deep theoretical investigation in the next future by means of a suitable theoretical/numerical model.

Table 9: Nonlinear jump effect, MIMO control and time history



To control the system vibrations in nonlinear field, an additional block has been added, see Figure 15, to prevent the immediate activation of the control. The forces and vibrations involved originate a strong control response that,

while not affecting control stability, can cause a shock impulsive response. In Figure 16 the time history presented shows the effect of the control with a forcing load of 9.5N, with and without the effect of the ramp; in particular, the signal sent to the actuator; in the time history of Figure 16a, a voltage peak is present, and the signal jumps up to 30V. The signal physically sent to the actuators, due to the software and hardware delimiter, was limited to the physical limit of the piezoelectric patches (+7.5/-2.5V before the amplifier, +1500/-500V to the actuators).

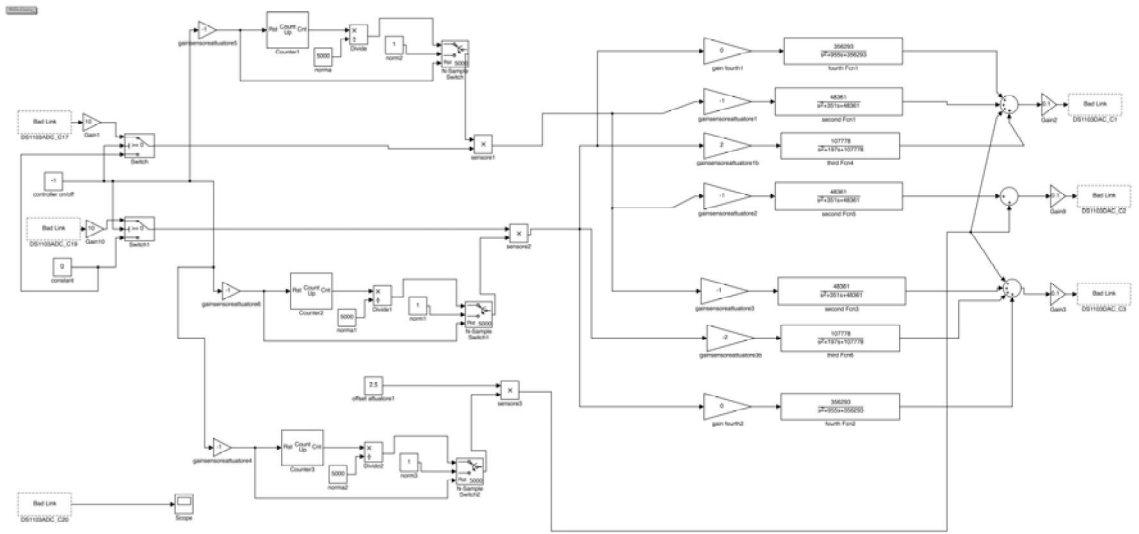


Figure 15: PPF MIMO nonlinear Simulink® block diagram

In order to prevent the unwanted impulsive peak, a linear ramp signal (between 0 and 1) with a duration of 1 second has been simply multiplied by the sensor signal to smooth the active control response activation. In Figure 16b the time history of the actuator of Figure 16a is shown, in Figure 18 the time history of the sensor and it can be noted how the activation of the control does not produce a shock response. Moreover, the robustness and the modal character of the control is also demonstrated by Figure 17, which shows the signal from the lower sensor. Without control, this presents

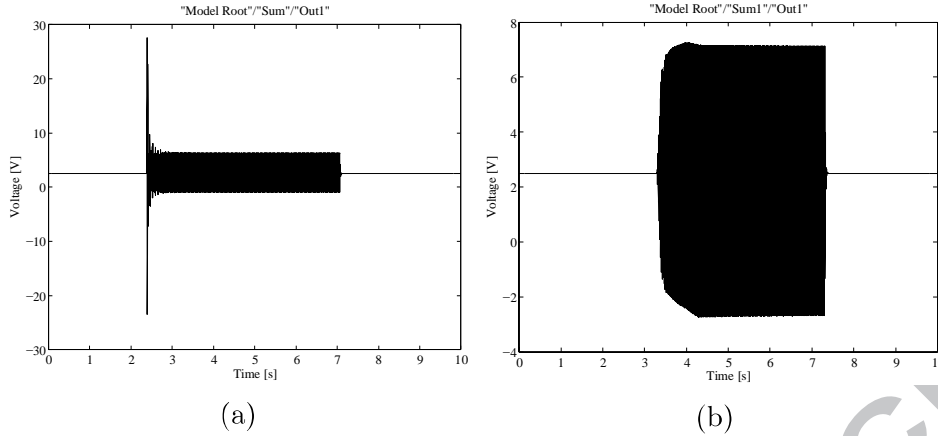


Figure 16: Actuator time history of Simulink[®] model (Figure 15) at forcing load 9.5 N: (a) without ramp, (b) with ramp

a clipping distortion when the signal exceeds a threshold of 1V, nevertheless, the control perfectly reduce the disturbance.

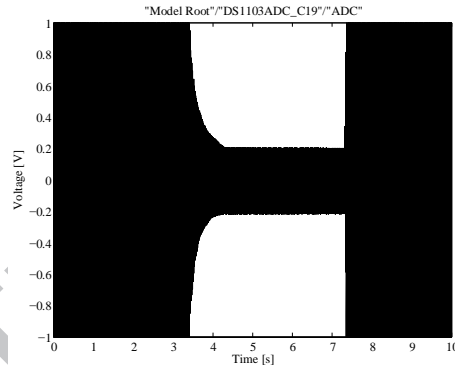


Figure 17: Time histories of Simulink[®] model at forcing load 9.5 N, Figure 15

In Figure 18 time histories of the Simulink[®] blocks are presented for the 5N forcing load sine test at 54.16Hz

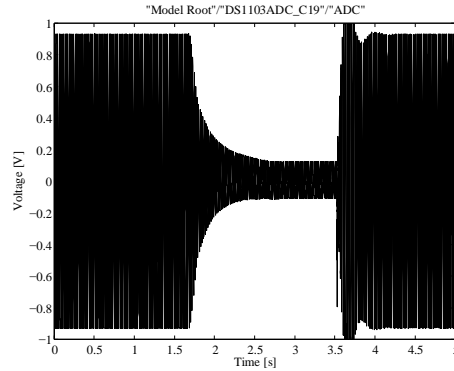


Figure 18: Time histories of Simulink[®] model at forcing load 5 N, Figure 15

6. Conclusion

In this paper an experimental setup has been developed to test the active vibration control of a free-edge rectangular sandwich plate. A control algorithm based on the Positive Position Feedback (PPF) technique has been successfully applied, using a digital dSPACE[®] controller board, with different combination of inputs/outputs (Single Input Single Output, MultiSISO, Multi Input Multi Output) to control the first four modes. The control is robust and efficient in reducing vibration amplitude in linear (small amplitude) and geometrically nonlinear (large amplitude vibrations), although the structure under investigation exhibits a high modal density in the studied range of 100Hz where four resonances are present. The proposed strategy allows to effectively control each resonance both individually or simultaneously. More tests need to be performed to better understand the nonlinear behaviour of the system and the electro-mechanic interactions of the different components.

References

- [1] T. Soong and G. Dargush, *Passive Energy Dissipation Systems in Structural Engineering*. Wiley, 1997.
- [2] M. J. Lam, D. J. Inman, and W. R. Saunders, "Vibration control through passive constrained layer damping and active control," *Journal*

- of Intelligent Material Systems and Structures*, vol. 8, no. 8, pp. 663–677, 1997.
- [3] J. Den Hartog, *Mechanical Vibrations*. Dover Civil and Mechanical Engineering, Dover Publications, 2013.
- [4] N. A. Alexander and F. Schilder, “Exploring the performance of a nonlinear tuned mass damper,” *Journal of Sound and Vibration*, vol. 319, no. 1–2, pp. 445 – 462, 2009.
- [5] F. Alijani, M. Amabili, G. Ferrari, and V. D’Alessandro, “Nonlinear vibrations of laminated and sandwich rectangular plates with free edges. part 2: Experiments and comparisons,” *Composite Structures*, vol. 105, no. 0, pp. 437 – 445, 2013.
- [6] F. Alijani and M. Amabili, “Nonlinear vibrations of laminated and sandwich rectangular plates with free edges. part 1: Theory and numerical simulations,” *Composite Structures*, vol. 105, no. 0, pp. 422 – 436, 2013.
- [7] R. Kumar, “Effective active vibration control of single link flexible manipulator with modified positive position feedback control in the presence of instrumentation phase lead/lag,” *Journal of Vibration and Control*, vol. 19, no. 10, pp. 1538–1560, 2013.
- [8] S. Carra, M. Amabili, R. Ohayon, and P. Hutin, “Active vibration control of a thin rectangular plate in air or in contact with water in presence of tonal primary disturbance,” *Aerospace Science and Technology*, vol. 12, no. 1, pp. 54 – 61, 2008. Aircraft noise reduction.
- [9] M. Zilletti, S. J. Elliott, P. Gardonio, and E. Rustighi, “Experimental implementation of a self-tuning control system for decentralised velocity feedback,” *Journal of Sound and Vibration*, vol. 331, no. 1, pp. 1 – 14, 2012.
- [10] M. K. Kwak, S. Heo, and M. Jeong, “Dynamic modelling and active vibration controller design for a cylindrical shell equipped with piezoelectric sensors and actuators,” *Journal of Sound and Vibration*, vol. 321, no. 3–5, pp. 510 – 524, 2009.

- [11] M. Friswell and D. Inman, "Relationship between positive position feedback and output feedback controllers," *Smart Materials and Structures*, vol. 8, no. 3, pp. 285–291, 1999. cited By (since 1996)75.
- [12] M. K. Kwak and S. Heo, "Active vibration control of smart grid structure by multiinput and multioutput positive position feedback controller," *Journal of Sound and Vibration*, vol. 304, no. 1–2, pp. 230 – 245, 2007.
- [13] S. Nima Mahmoodi, M. Ahmadian, and D. J. Inman, "Adaptive modified positive position feedback for active vibration control of structures," *Journal of Intelligent Material Systems and Structures*, vol. 21, no. 6, pp. 571–580, 2010.
- [14] E. Omid and S. N. Mahmoodi, "Vibration control of collocated smart structures using h^∞ modified positive position and velocity feedback," *Journal of Vibration and Control*, 2014.
- [15] J. Fanson and T. Caughey, "Positive position feedback control for large space structures," *AIAA Journal*, vol. 28, no. 4, pp. 717–724, 1990. cited By (since 1996)372.
- [16] W. El-Ganaini, N. Saeed, and M. Eissa, "Positive position feedback (ppf) controller for suppression of nonlinear system vibration," *Nonlinear Dynamics*, vol. 72, no. 3, pp. 517–537, 2013.
- [17] E. Pereira and S. S. Aphale, "Stability of positive-position feedback controllers with low-frequency restrictions," *Journal of Sound and Vibration*, vol. 332, no. 12, pp. 2900 – 2909, 2013.
- [18] Y. Li, J. Onoda, and K. Minesugi, "Simultaneous optimization of piezoelectric actuator placement and feedback for vibration suppression," *Acta Astronautica*, vol. 50, no. 6, pp. 335–341, 2002. cited By (since 1996)31.
- [19] P. Liu, V. Rao, and M. Derriso, "Active control of smart structures with optimal actuator and sensor locations," in *Proceedings of SPIE - The International Society for Optical Engineering*, vol. 4693, pp. 1–12, 2002. cited By (since 1996)11.
- [20] L. Beranek, *Noise and vibration control*. McGraw-Hill, 1971.

- [21] A. Moulson and J. Herbert, *Electroceramics: Materials, Properties, Applications*. Springer, 1990.
- [22] C. Fuller, S. Elliott, and P. Nelson, *Active Control of Vibration*. Academic Press, 1997.
- [23] “<http://www.smart-material.com>.”
- [24] “http://www.kemo.com/kemohtml/cardmaster21_255g.shtml.”
- [25] C. Goh and T. Caughey, “On the stability problem caused by finite actuator dynamics in the collocated control of large space structures.” *International Journal of Control*, vol. 41, no. 3, pp. 787–802, 1985. cited By (since 1996)189.